

Temporal evolution and correlation between cooperative luminescence and photodarkening in ytterbium doped silica fibers

Hrvoje Gebavi,^{1*} Stefano Taccheo,¹ Daniel Milanese,² Achille Monteville,³ Olivier Le Goffic,³ David Landais,³ David Mechin,³ Denis Tregcoat,³ Benoit Cadier,⁴ and Thierry Robin⁴

¹College of Engineering, Swansea University, Singleton Park, SA2 8PP, Swansea, UK

²Politecnico di Torino, Dipartimento di Scienza dei Materiali ed Ingegneria Chimica, Corso Duca degli Abruzzi 24, 10129, Torino, Italy

³Perfos, 11 rue Louis de Broglie, F-22300 Lannion, France

⁴iXFiber S.A.S., Rue Paul Sabatier, F-22300 Lannion, France

*h.gebavi@swansea.ac.uk

Abstract: The present work describes photodarkening from the viewpoint of cooperative luminescence. The temporal evolution of both effects was measured simultaneously by means of ytterbium doped aluminosilicate fibers for concentrations up to 1.8 wt% Yb³⁺. The quadratic dependence of photodarkening and cooperative luminescence versus dopant concentration was observed. The change in the photodarkening and cooperative luminescence mutual dynamics for highly and low doped fibers is ascribed to a different ion number which forms the cluster. Cooperative luminescence is proved to be a natural probe for photodarkening since it provides new pieces of information and contributes to the photodarkening mechanism description.

©2011 Optical Society of America

OCIS codes: (140.3510) Lasers, fiber; (160.5690) Rare-earth-doped materials; (260.5210) Photoionization; (140.3615) Lasers, ytterbium.

References and links

1. R. Paschotta, J. Nilsson, P. R. Barber, J. E. Caplen, A. C. Tropper, and D. C. Hanna, "Lifetime quenching in Yb-doped fibres," *Opt. Commun.* **136**(5-6), 375–378 (1997).
2. M. Engholm, L. Norin, and D. Åberg, "Strong UV absorption and visible luminescence in ytterbium-doped aluminosilicate glass under UV excitation," *Opt. Lett.* **32**(22), 3352–3354 (2007).
3. J. Kirchhof, S. Unger, A. Schwuchow, S. Grimm, and V. Reichel, "Materials for high-power fiber lasers," *J. Non-Cryst. Solids* **352**(23-25), 2399–2403 (2006).
4. G. R. Atkins and A. L. G. Carter, "Photodarkening in Tb³⁺-doped phosphosilicate and germanosilicate optical fibers," *Opt. Lett.* **19**(12), 874–876 (1994).
5. M. M. Broer, D. M. Krol, and D. J. Digiovanni, "Highly nonlinear near-resonant photodarkening in a thulium-doped aluminosilicate glass fiber," *Opt. Lett.* **18**(10), 799–801 (1993).
6. P. Laperle, A. Chandonnet, and R. Vallée, "Photoinduced absorption in thulium-doped ZBLAN fibers," *Opt. Lett.* **20**(24), 2484–2486 (1995).
7. E. Nakazawa and S. Shionoya, "Cooperative Luminescence in YbPO₄," *Phys. Rev. Lett.* **25**(25), 1710–1712 (1970).
8. S. Magne, Y. Ouerdane, M. Druetta, J. P. Goure, P. Ferdinand, and G. Monnom, "Cooperative luminescence in an ytterbium-doped silica fiber," *Opt. Commun.* **111**(3-4), 310–316 (1994).
9. R. S. Brown, W. S. Brocklesby, W. L. Barnes, and J. E. Townsend, "Cooperative energy transfer in silica fibres doped with ytterbium and terbium," *J. Lumin.* **63**(1-2), 1–7 (1995).
10. B. Schaudel, P. Goldner, M. Prassas, and F. Auzel, "Cooperative luminescence as a probe of clustering in Yb³⁺ doped glasses," *J. Alloy. Comp.* **300–301**, 443–449 (2000).
11. S. Yoo, C. Basu, A. J. Boyland, C. Sones, J. Nilsson, J. K. Sahu, and D. Payne, "Photodarkening in Yb-doped aluminosilicate fibers induced by 488 nm irradiation," *Opt. Lett.* **32**(12), 1626–1628 (2007).
12. P. D. Dragic, C. G. Carlson, and A. Croteau, "Characterization of defect luminescence in Yb doped silica fibers: part I NBOHC," *Opt. Express* **16**(7), 4688–4697 (2008).
13. A. D. Guzman Chávez, A. V. Kir'yanov, Y. O. Barmenkov, and N. N. Il'ichev, "Reversible photo-darkening and resonant photobleaching of Ytterbium-doped silica fiber at in-core 977-nm and 543-nm irradiation," *Laser Phys. Lett.* **4**(10), 734–739 (2007).

14. L. Dong, "Advanced Specialty Fibers for Applications in Fiber Lasers," Advanced solid-state photonics, OSA Technical Digest (CD) (Optical Society of America, 2011), paper JWA1.
15. S. Jetschke, M. Leich, S. Unger, A. Schwuchow, and J. Kirchof, "Influence of Tm- or Er-codoping on the photodarkening kinetics in Yb fibers," *Opt. Express* **19**(15), 14473–14478 (2011).
16. S. Taccheo, H. Gebavi, A. Monteville, O. Le Goffic, D. Landais, D. Mechin, D. Tregoat, B. Cadier, D. Milanese, and T. Robin, "Concentration dependence and self-similarity of photodarkening losses induced in Yb-doped fibers by comparable excitation," *Opt. Express* **19**, 19340–19345 (2011).
17. T. G. Ryan and S. D. Jackson, "Cooperative luminescence and absorption in ytterbium doped aluminosilicate glass optical fibres and preforms," *Opt. Commun.* **273**(1), 159–161 (2007).
18. S. Jetschke, S. Unger, A. Schwuchow, M. Leich, and J. Kirchof, "Efficient Yb laser fibers with low photodarkening by optimization of the core composition," *Opt. Express* **16**(20), 15540–15545 (2008).
19. Y. G. Choi, Y. B. Shin, H. S. Seo, and K. H. Kim, "Spectral evolution of cooperative luminescence in an Yb³⁺-doped silica optical fiber," *Chem. Phys. Lett.* **364**(1-2), 200–205 (2002).
20. A. V. Kir'yanov, Y. O. Barmenkov, I. L. Martinez, A. S. Kurkov, and E. M. Dianov, "Cooperative luminescence and absorption in Ytterbium-doped silica fiber and the fiber nonlinear transmission coefficient at $\lambda=980$ nm with a regard to the Ytterbium ion-pairs' effect," *Opt. Express* **14**(9), 3981–3992 (2006).
21. S. Jetschke, S. Unger, U. Röpke, and J. Kirchof, "Photodarkening in Yb doped fibers: experimental evidence of equilibrium states depending on the pump power," *Opt. Express* **15**(22), 14838–14843 (2007).
22. J. Kirchof, S. Unger, S. Jetschke, A. Schwuchow, M. Leich, and V. Reichel, "Yb doped silica based fibers: Correlation of photodarkening kinetics and related optical properties with the glass composition," *Proc. SPIE* **7195**, 71950S (2009).
23. C. G. Carlson, K. E. Keister, P. D. Dragic, A. Croteau, and J. G. Eden, "Photoexcitation of Yb-doped aluminosilicate fibers at 250 nm: evidence for excitation transfer from oxygen deficiency centers to Yb³⁺," *J. Opt. Soc. Am. B* **27**(10), 2087–2094 (2010).

1. Introduction

The photodarkening effect [1] (PD) is considered to be the critical factor for high power fiber lasers and amplifiers power stability [2, 3]. It is observed in silica based glass matrixes doped with various rare earth ions (Tb³⁺, Tm³⁺, Yb³⁺) [4–6]. In the case of Yb doping, the NIR emission at $\sim 1 \mu\text{m}$ is usually accompanied by a visible green emission.

The green luminescence of Yb³⁺ at ~ 500 nm has been noticed for the first time in 1970, well before PD became an issue, and determined as the emission of a photon by a pair of excited ions in cooperation [7]. In the fiber geometry, Yb³⁺ cooperative luminescence (CL) is well described by the power-law modeling [8] and related to clustering [9, 10]. As it is reported, CL power is six orders of magnitude lower than infrared single – ion fluorescence power, and it shows quadratic dependence on infrared – excitation power [8], with a half lifetime value of a single Yb³⁺ luminescence [7].

The PD creation mechanism is still under debate [2, 11, 12]. In fact, at first sight, it is featured by color centers generation and UV luminescence [13]. CL may create higher energetic photons, possibly in the UV wavelength range, which could be responsible or contribute to the PD effect through color center formation [14]. The investigation of CL could therefore provide an insight on the PD mechanism. To illustrate the point it may be noted that the visible emission of Er and Tm contaminated aluminosilicate fibers was recently scrutinized [15].

The aim of the present paper is to investigate the relationship among CL and PD in order to improve understanding of PD. Both effects were measured simultaneously for various dopant concentrations.

2. Experimental

Aluminosilicate fibers with 0.5, 0.9, 1, 1.075, 1.35, 1.8 wt% Yb³⁺ dopant concentrations were fabricated by mean of the modified chemical vapor deposition (MCVD) technique. Short fiber samples (0.2 – 20 cm) with a similar core radius of $\sim 6.6 \mu\text{m}$ were tested in a 24 hour period. Constant inversion of $\sim 46\%$ was achieved by utilizing short fiber lengths, and the different dopant concentrations were adjusted in order to obtain the same total number of Yb³⁺ [16]. The pump and HeNe - probe powers were ~ 200 mW and $\sim 0.5 \mu\text{W}$, respectively. The experimental setup utilized for PD and CL examination is shown in Fig. 1.

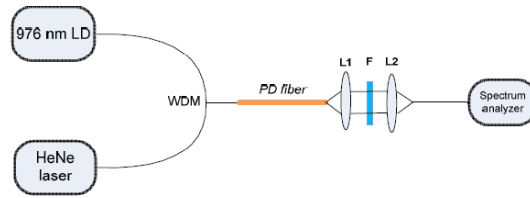


Fig. 1. Experimental setup used to carry out PD and CL temporal evolution measurements simultaneously ('L1', 'L2' are collimating lenses, 'F' signs filter for 976 nm laser diode 'LD').

The HeNe laser at 633 nm and 976 nm LD pump beams are coupled into a tested fiber by customized 980nm/633nm combiner (WDM) developed by one of the co-authors in order to improve the stability of 633 nm probe. The combiner was spliced to the fibers and the output emission is first collimated and then focused into a collecting fiber connected with a spectrum analyzer. The spectrum analyzer is an array of CCD covering the 200 nm – 1100 nm interval. The free space path is useful to filter out the residual pump power. The experimental setup, built in the way cited herein, enables the simultaneous monitoring of PD and CL temporal evolution at 633 nm by using the HeNe laser as a probe and green luminescence at ~500 nm.

The green luminescence depends on the Al^{3+} content [17] as well as PD [18]. In the present study, the Al^{3+} content was varying as the Yb^{3+} dopant concentration was increasing in the following sequence: 1.8, 3.2, 3.4, 3.2, 3.2, 1.8 wt% Al^{3+} . It is assumed that the variations in the Al^{3+} content do not significantly influence the presented results. Detailed study of Al^{3+} content impact will be provided in following papers.

The impurities, such as Er^{3+} and Tm^{3+} ions, can give their contribution to CL by emitting photons at ~537 and 470 nm, respectively [17]. In the study in question no contamination from impurities were observed.

3. Cooperative luminescence and NIR ytterbium emission dependence

In the course of this investigation, before monitoring temporal evolution of CL due to PD, it is appropriate to examine the relationship between CL and Yb^{3+} emission in the NIR region.

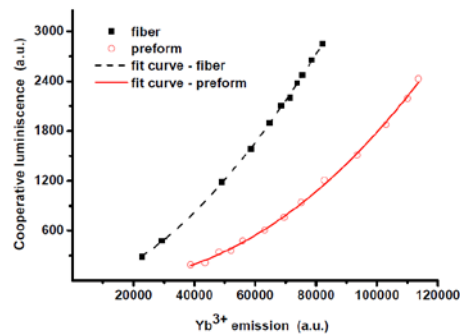


Fig. 2. Integrated intensity of CL and Yb^{3+} NIR emission. Fiber length is 2 mm and preform slice thickness 0.5 mm. Experimental results were fitted on power function and the obtained exponents were: $p_{\text{fiber}} = (1.69 \pm 0.05)$, $p_{\text{preform}} = (2.21 \pm 0.09)$.

The emission of one photon at ~500 nm requires two simultaneously de-excited Yb^{3+} neighboring ions and therefore quadratic mutual dependence should be expected. Two experiments were performed, the first one on a 2 mm long fiber and the second one on a 0.5 mm thick preform slice. As a consequence, samples had a short interaction length in order to minimize reabsorption, a different geometry and the same Yb^{3+} concentration of 1.8 wt%. Before carrying out the experiments, PD in both samples was in its final, equilibrium state. Green luminescence has very weak intensity and due to the fact the experiments were made in frontal geometry. Integrated intensity of CL and Yb^{3+} NIR emission for various pump powers is presented in Fig. 2.

Less-than-square and overestimated values discrepancy from quadratic dependence in fiber together with preform interaction geometry are observed. However, the results fluctuations are less than 15% of the expected value. A similar breaking of quadratic low dependence among CL and pump power is reported in highly doped silica fibers [19, 20]. The results were described as the consequence of fibers lengths and amplified spontaneous emissions (ASE) which had an influence in the presented experiments as well.

4. Photodarkening and cooperative luminescence temporal evolution

Figure 3 shows an example of the CL (~500 nm) spectra and the HeNe probe at 633 nm used for PD monitoring in time.

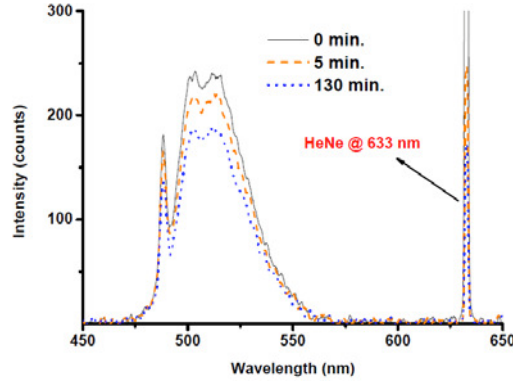


Fig. 3. Characteristic temporal emission spectra of the 1.8 wt% Yb³⁺ doped fiber and the PD - probe at 633 nm.

To evaluate the temporal dependence of CL and its relationship with PD we measured the PD excess loss at both 513 and 633 nm (Fig. 3). On the ordinate axis of Fig. 4a, and b the excess loss at 513 and 633 nm normalized to the final excess loss value is presented. However, the origin of the loss is different. On the one hand, the decrease of the 633 nm probe is due to the generation of PD losses until the final equilibrium loss is reached [16]. On the other hand, CL photons are generated within the fiber. It is possible to assume that its generation is uniform within the fiber since the Yb³⁺ inversion is uniform as well. The second assumption considers that the generation rate is constant in time during the PD evolution. Both assumptions were verified to be true, within our resolution limits, testing fibers and preform samples. As a result, in both, CL and PD – probe at 633nm, there is an effect of PD induced losses. Nevertheless, the CL emitted at the fiber beginning will travel longer and suffer the highest PD loss while propagating towards the end. This can be summarized as follows:

$$R_{633} = \frac{I_{633}(t)}{I_{633}(0)} = e^{-\alpha_{633}(t) \cdot L} \quad (1)$$

$$R_{513} = \frac{I_{513}(t)}{I_{513}(0)} = \frac{1}{L} \int_0^L e^{-\alpha_{513}(t)(z-L)} dz = \frac{1 - e^{-\alpha_{513}(t) \cdot L}}{\alpha_{513}(t) \cdot L} \quad (2)$$

where α_λ is the absorption coefficient related to PD induced losses at wavelength λ .

Figures 4a and 4b show the characteristic temporal evolution of the PD probe at 633 nm and CL intensity at 513 nm for 0.5 and 1.35 wt% Yb³⁺ doped samples. Experimental data were fitted on the stretched exponential curve [16] and normalized to its final value.

Figure 4a shows that CL and PD evolve in time in a similar way. Nonetheless, it is not the case of highly doped samples (Fig. 4b). They progress equally up to around 30% of their total amplitude decay. In the following step the rate changes and quadratic dependence is observed

before reaching the equilibrium state. As a result, CL vs. PD dependence has changed from linear to quadratic (Fig. 5) for dopant concentrations range from 0.5 to 1.35 wt%. The indicated rate change may be defined by mean of a different number of cluster participants. As to the low doped case (0.5 wt% Yb^{3+}) it is possible to assume that two Yb^{3+} ions create a pair, whilst concerning the highly doped case (1.35 wt% Yb^{3+}) four Yb^{3+} ions contribute in the cluster creation. The previously cited observation is supported by the necessity of 3 [16] to 3.5 [21] excited Yb^{3+} ions for the color center creation. As a consequence, the difference in the temporal evolution dynamic between low and highly doped samples may be explained by using clusters composed of a different number of ytterbium ions. Furthermore, this issue could be coherent with the assumption of higher CT states excitation and corresponding 230 nm absorption band shift toward lower wavelengths due to the cluster numbers increase [2].

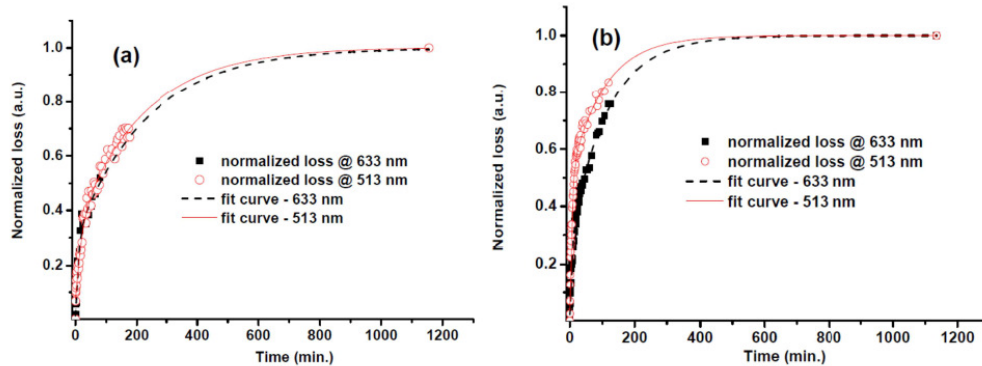


Fig. 4. (a) The temporal evolution of CL at 513 nm and PD probe at 633 nm for the sample doped with 0.5 wt% Yb^{3+} normalized on its final value; (b) CL and 633 nm probe temporal evolution for 1.35 wt% Yb^{3+} doped fiber sample.

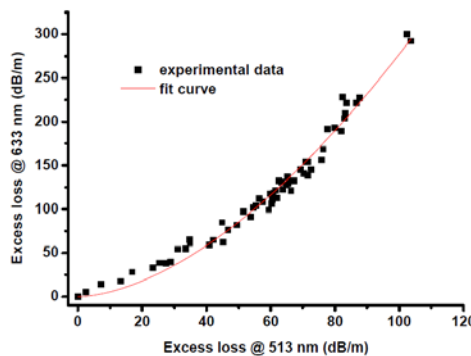


Fig. 5. CL and PD at 633 nm dependence in time. Excess loss values are processed by Eqs. (1) and 2. The fiber sample is doped with 1.35 wt% Yb^{3+} . The power fit curve has a 1.70 ± 0.04 exponent coefficient.

5. Photodarkening and cooperative luminescence correlation with dopant concentration

The obtained results of PD and CL excess loss showed a quadratic dependence on the Yb^{3+} concentration (Fig. 6). It is already reported that PD linearly depends on population inversion [21]. In the present study, dopant concentration was changed whilst keeping the inversion approximately the same as described above. The quadratic dependence of CL with dopant concentration was assumed in Yb^{3+} doped aluminosilicate fibers [22]. The presented experimental data highlight the fact that the dependence remains even when the PD loss is

monitored. Therefore, the PD loss at 513 and 633 nm has the same quadratic dependence with dopant concentration for the examined set of samples.

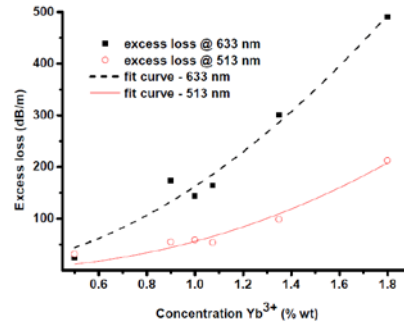


Fig. 6. Excess loss for different Yb³⁺ concentrations. The obtained power fit exponents are: $p_{633} = (1.9 \pm 0.2)$, and $p_{513} = (2.2 \pm 0.2)$.

The lower value of PD excess loss values at 513 nm is surprising since PD losses increase as the wavelength decreases. A possible explanation (see Eq. (2)) is that the emission rate of green luminescence increases as the PD process proceeds. However, we have monitored this effect for 24h in performs and have not observed any increase of green luminescence. The second explanation of the low green light loss can lay in the fact that green light is scattered and guided in the cladding and therefore less PD related loss was observed. Because of that, the additional experiment with the single mode fiber spliced to the testing fiber output was prepared. The obtained results did not show significant deviations from the presented results. In author's opinion, the question of the low green luminescence loss seems to reside in a simultaneous electron – hole recombination process i.e. a kind of self - bleaching in the selected region. The claim adopted here is based on observation of the partial bleaching in Yb³⁺ doped fibers obtained by 543 nm laser beam [13]. Nevertheless, our hypothesis remains an open question.

Photo-induced optical damage may originate from an electron release of a ligand neighboring an excited Yb³⁺ pair, followed by an absorption and correspondent emission in the recombination process [13]. The cluster number, indicated by the area under the CL emission in the present study, decreases in time which goes in parallel with Yb³⁺ → Yb²⁺ transformation if the charge transfer (CT) as the main PD mechanism is supposed. Hence, it is possible to affirm that the self – trapping mechanism of CL could be influenced by the increase in Yb²⁺ and correspondent whole centers number.

In answer to the question addressed in the introduction, it can be concluded that CL loss may play a role in the PD process whether being an intermediate state necessary to reach CT band [2] or giving the internal excitation to the oxygen deficiency centers (ODC) [23]. Here we can frame an extension of the paradigm by including a kind of self – bleaching process of CL as stated above.

6. Conclusion

Up to the current knowledge, for the first time the PD and CL excess losses are measured simultaneously in time. The temporal evolution of PD and CL show different dynamics for low and high doped samples. Excess loss rates in the low doped samples are similar whilst in the highly doped samples significant rate change is observed. The change in dynamic described herein may be related to a different clustering amount. The CL loss that is observed is lower than expected. This may suggest an interplay of the CL light with the material. In conclusion, the quadratic dependence of PD at 633 nm and CL loss at 513 nm on dopant concentration is demonstrated and possible consequences of CL on PD are discussed.

Acknowledgments

This project was funded by FP7 LIFT (Leadership in Fiber Technology) Project (Grant #228587).